IIETA International Information and Engineering Technology Association
Advancing the World of Information and Engineering

Annales de Chimie - Science des Matériaux
Vol. 46, No. 3, June, 2022, pp. 147-154
Journal homepage: http://iieta.org/journals/acsm

# Valorisation of Industrial Soda-Lime Glass Waste and Its Effect on the Rheological Behavior, Physical-Mechanical and Structural Properties of Sanitary Ceramic Vitreous Bodies

Khaled Boulaiche[1*], Kamel Boudeghdegh[1], Sofiane Haddad[2], Abdelmalek Roula[3], Hichem Alioui[4]

[1] Laboratory of Applied Energetics and Materials (LEAM), Faculty of Sciences and Technology, University of Mohammed Seddik Ben Yahia, Jijel 18000, Algeria
[2] Renewable Energy Laboratory, Faculty of Sciences and Technology, University of Mohammed Seddik Ben Yahia, Jijel 18000, Algeria
[3] Laboratory of Interactions Material-Environment (LIME), Faculty of Sciences and Technology, University of Mohammed Seddik Ben Yahia, Jijel 18000, Algeria
[4] Laboratory of Civil Engineering and Environment (LCEE), Faculty of Sciences and Technology, University of Mohammed Seddik Ben Yahia, Jijel 18000, Algeria

Corresponding Author Email: khaledboulaiche@univ-jijel.dz

https://doi.org/10.18280/acsm.460306

**Received:** 24 April 2022
**Accepted:** 28 May 2022

***Keywords:***
*SLGW, sanitary VC body, physical properties, flexural strength*

**ABSTRACT**

In this study, the effect of substitution of feldspar by soda-lime glass waste (SLGW), on rheological behavior, thermal, physical-mechanical and structural properties of sanitary-ware vitreous china (VC) bodies, has been evaluated. The findings show a positive effect on the rheological behavior of the slip, to viscosity, thixotropy, density and casting process. Indeed, during the firing stage at 1230°C, the use of 20 wt. % of SLGW in the composition of VC bodies, improved Bulk density (2 to 2.52 g/cm$^3$), reduced water absorption (0.35 to 0.02%), and increased flexural strength (33 to 51 MPa). The fired samples were characterized using X-ray diffraction, SEM and FTIR analysis; results indicate that Mullite and Quartz are the major phases, with a little presence of anorthite phase formed by SLGW additions. From TGA/DTG analysis, it was found that the use of SLGW (15 wt. %) reduces mass loss of VC bodies (8.83 to 8.53%). These positive results open new horizons for using this waste, as a sound environmental, technological and economic solution.

## 1. INTRODUCTION

Evidently, among ceramics, Sanitary ceramic is one of the most significant types of ceramics due to its high technical characteristics; it is mainly used in the building industry [1]. Indeed, demand for various ceramic products is increasing [2]. Mostly, the production of sanitary-ware VC bodies, is based on the preparation of slip; the raw materials used in slip formulation are in general a mix of kaolin (25-35%), clay (20-28%), feldspar (15-23%) and quartz (17-31%). In the manufacturing process of sanitary VC bodies, a series of parameters must be respected; in particular, we must ensure good rheological properties to allow the casting: Gallenkamp viscosity of about 300-330 °G, thixotropy after 1 min at about 20-30 °G, and a thickness, after 60 min, of at least 0.7cm [3]. Following this, the ceramic bodies are dried and spray-glazed in order to enhance their various chemical-mechanical properties [4-6]. Finally, they are fired in the kiln. During the firing cycle, the ceramic bodies undergo physical-chemical changes, as demonstrated by many studies conducted by several authors [7, 8]. The quality of final product of course, depends on the properties of raw materials and the firing conditions [9, 10]. Generally, the principal phases in VC bodies are: glassy phase, mullite and residual quartz. Mullite is the main constituent it has a low expansion coefficient and a high strength; this allows improvement in the technical characteristics of the ceramic products [11-13].

Recently, the increase in ceramic bodies production worldwide, warns about the depletion of raw materials resources over time. For these reasons, the research community is attempting to find new resources that satisfy the standards of the ceramic industry; as an example, they are focusing on the study of the possibility of recycling and incorporating industrial waste into various ceramic formulations. The recycling of these wastes can help reduce the depletion of natural raw materials and reduce pollution. In this context, many types of ceramics have been prepared from various industrial wastes. These are mainly: blast furnace slag [14, 15], solid ceramic waste [16], fly ash [17-19], red mud [20], Glass Frit [21] and glass waste [22-25].

SLGW has a similar chemical composition as feldspar and present the same behavior during the firing process [26]. From previous studies, the partial or total replacement of feldspar by SLGW accelerates the densification process, and reduces the firing temperature from 1340°C to 1240°C, without affecting the slip casting parameters [27, 28]. Also, the plastic deformation is reduced when 6wt. % of feldspar are replaced by SLGW, in porcelain stone ware tile body; this helps to close the pores and reduce water absorption to 0.2% at 1080°C [26]. On the other hand, mullite growth kinetics, become faster by the substitution of feldspar by SLGW (from 7 to 30 wt. %) in vitreous ceramics. The reduction of the firing temperature by

70 to 100°C, mentioned previously contributes to energy saving and the reduction of carbon dioxide emissions [29].

The rich content of $SiO_2$, $Na_2O_3$ and CaO in soda-lime glass waste (SLGW), as industrial waste, the limited knowledge about its use in the sanitary ceramics industry. The novelty in this study is the potential use of SLGW as a partial substitute for two types of feldspar (Na + K) in the sanitary ware body composition. The first part of this work aims at controlling the rheological behaviour of the slip ceramic by the use of Na-electrolytes. The purpose of the second part is to define the optimum composition (from 5 up to 20 wt. %) for obtaining better physical-mechanical and structural properties of fired ceramics. This investigation contributes to compensating for the depletion of natural raw materials, leads to significant economic by getting a less expensive ceramic body and reducing environmental pollution with various technical benefits (improving the physical-mechanical properties, decreasing the firing temperature).

## 2. MATERIALS AND METHODS

### 2.1 Raw materials

**Table 1.** Formulations (in wt. %) of batch compositions VC, C2, C3, C4 and C5

| Raw material | VC | C2 | C3 | C4 | C5 |
|---|---|---|---|---|---|
| Clay (Hycast VC) | 28 | 28 | 28 | 28 | 28 |
| Par Kaolin | 12 | 12 | 12 | 12 | 12 |
| kaolin RMB | 12 | 12 | 12 | 12 | 12 |
| Na- feldspar | 12 | 9.5 | 7 | 4.5 | 2 |
| K- feldspar | 11 | 8.5 | 6 | 3.5 | 1 |
| Quartz | 25 | 25 | 25 | 25 | 25 |
| SLGW | 0 | 5 | 10 | 15 | 20 |

**Table 2.** Chemical analysis of the raw materials

| Oxides | Clay VC | Par kaolin | kaolin RMB | Na feldspar | K feldspar | Quartz | SLGW |
|---|---|---|---|---|---|---|---|
| $SiO_2$ | 52 | 48 | 48 | 70.74 | 69.5 | 96.35 | 70.25 |
| $Al_2O_3$ | 31 | 37 | 37 | 17.92 | 17.3 | 0.52 | 1.71 |
| $TiO_2$ | 1 | 0.06 | 0.05 | 0.26 | 0 | 0.05 | 0 |
| CaO | 2 | 0.07 | 0.07 | 0.5 | 0.5 | 1.19 | 13.43 |
| MgO | 0.4 | 0.3 | 0.3 | 0.2 | 0.2 | 0.08 | 0.52 |
| $K_2O$ | 2.1 | 1.9 | 1.75 | 0.4 | 9 | 0.17 | 0.28 |
| $Na_2O$ | 0.2 | 0.1 | 0.1 | 9.6 | 3.5 | 0.08 | 13.43 |
| $Fe_2O_3$ | 1.2 | 0.19 | 0.8 | 0.08 | 0.16 | 0.24 | 0.33 |
| L.O.I | 12 | 11.8 | 12.1 | 0.5 | 0.4 | 1.2 | 0.1 |

**Table 3.** Chemical analysis of slip modified by SLGW

| Oxides | VC | C2 | C3 | C4 | C5 |
|---|---|---|---|---|---|
| $SiO_2$ | 70.21 | 70.21 | 70.22 | 70.22 | 70.23 |
| $Al_2O_3$ | 24.15 | 23.35 | 22.56 | 21.76 | 20.97 |
| $TiO_2$ | 0.37 | 0.37 | 0.36 | 0.35 | 0.35 |
| CaO | 0.49 | 1.14 | 1.79 | 2.43 | 3.08 |
| MgO | 0.27 | 0.29 | 0.30 | 0.32 | 0.33 |
| $K_2O$ | 2.24 | 2.02 | 1.80 | 1.58 | 1.36 |
| $Na_2O$ | 1.77 | 2.11 | 2.46 | 2.80 | 3.14 |
| $Fe_2O_3$ | 0.61 | 0.62 | 0.63 | 0.64 | 0.65 |

The raw materials used for the preparation of the VC bodies: Hycast VC ball clay from UK. Two types of kaolin were used; the first, kaolin Remblend denoted as RMB (IMERYS Ceramics, Austell, UK) and the second type named Parkaolin (IMERYS Minerals Ltd, UK). Quartz is derived from deposits in Bir el-Ater (Tebessa, Algeria). Sodium and potassium feldspar are from Çine (Aydin, Turkey). SLGW powder comes from the factory of the African Glass Company (Jijel, Algeria). In a tunnel kiln, small quantities of SLGW and feldspar were fired at 1230°C in order to investigate their melting behavior. Loss of ignition (L.O.I) was determined by firing at 1000°C for 2 hours. Five compositions of VC bodies were prepared; we have a reference sample, which is SLGW free, defined as VC (0 wt. % SLGW). Concerning the following four, we have the gradual replacement of feldspar by SLGW. The compositions of ceramic bodies, are presented in Table 1 (in weight %). The chemical compositions of the raw materials, were obtained by an X-ray fluorescence spectrometer Rigaku ZSX Primus IV (see Table 2). The slips compositions are summarized in Table 3.

### 2.2 Samples preparation

To prepare sanitary VC bodies, the first step is to prepare the slip by diluting clay with 15wt. % water in a mill equipped with alumina balls; then, the quartz is ground up to obtain particles with a diameter under 63µm. Crushed sand and diluted clay are mixed with feldspar and kaolin with an adequate amount of water. The mixture is then, milled in a ceramic jar for 4 hours at 120 rpm, to obtain the residue on a sieve of 63 µm (less than 2%). To improve the milling efficiency, small quantities of deflocculating agents: sodium carbonate and sodium silicate (high Purity: 99.9%, grade ACS reagent), were added to the slip before mixing.

Figure 1 illustrates the manufacturing steps. The industrial slip density is, generally, in the range of 1.77-1.79 g/cm$^3$. Slip fluidity was measured by calculating the time required to pass the slip through a ford cup 100ml (2.6 mm opening). Slip viscosity is measured using a universal torsion viscometer (mod.TV/30/A, Gallenkamp type). The thicknesses during casting, were measured according to time steps of 10, 30, and 60 minutes. The obtained slip was poured into rectangular plaster moulds, at room temperature. In each mixture 8 test pieces (70×20×10mm), were prepared to measure water absorption, rectangular samples (120×20×20mm) were prepared to measure both linear shrinkage and flexural strength. The samples were then dried at room temperature for 48 hours, then, at 105°C for 8 hours. The green bodies were fired in a tunnel kiln, for 21 h, at a maximum temperature of 1230°C, under industrial conditions.

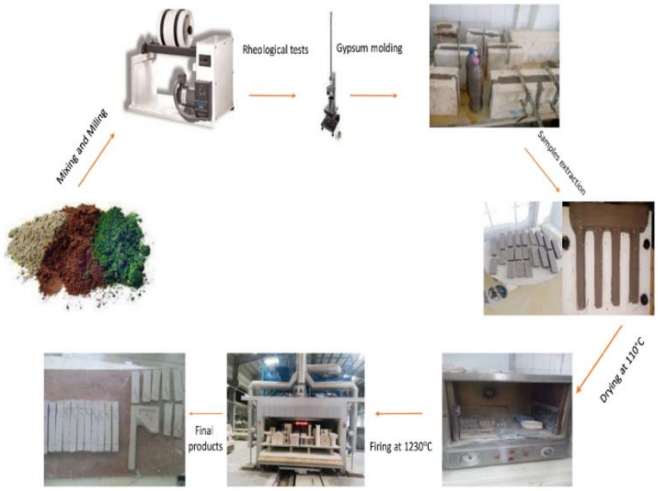


**Figure 1.** Manufacturing steps of sanitary VC bodies

### 2.3 Methods of characterization

The thermal behavior of green ceramics was characterized by thermogravimetry analysis (TGA/DGA), using the equipment (TGA-DSC, Universal V4.5A TA Instruments) for temperatures up to 1300°C, with a heating rate of 5°C / min in air atmosphere. Alumina powder was used as reference material.

X-ray diffraction (XRD) was performed to determine the crystal phases of the fired samples on a Siemens D5000 diffractometer, using Cu-kα (λ = 1.5406 Å) radiation in the Bragg Brentano configuration, X-ray patterns recordings 2θ range from 5 to 100 degrees, The quantitative analysis of phase percentages was obtained, using X-Pert High Score software.

To characterize the morphology of crystal particles and the microstructure of the samples, a Scanning Electron Microscope (SEM) (WD S, JEOL JSM 6360LV) has been used.

The infrared transmission spectra were extracted using sample powder burnt into KBr pellets (purity: 99.9%, Spectral quality). The data was registered by spectrophotometer of Shimadzu Japan, in the interval 4000-500 $cm^{-1}$.

Some physical and mechanical properties of fired bodies, were experimentally characterized; the bulk density ($D_B$) was determined by Archimedes' procedure; the true density ($D_T$) using the densimeter Candlot- Le Chatelier and the total porosity P (%) is calculated by Eq. (1)

$$P\ (\%) = \frac{(D_T - D_B)}{D_T} * 100 \quad (1)$$

The water absorption (WA) is determined using the following procedure: the dried samples are weighed (m0), and after immersion for 2 hours in boiling water, cooled for 12 hours. Then, the surface is dried with a wet towel (m1) then, the samples are weighed second time.

The water absorption is calculated using Eq. (2).

$$WA\ (\%) = \frac{(m1 - m0)}{m0} * 100 \quad (2)$$

The value of linear shrinkage (LS) is determined by calculating the difference between lines inscribed on the samples before and after firing, a specified length (10 cm) being recorded before firing $L_i$ and after firing $L_f$. The linear shrinkage is calculated by Eq. (3)

$$LS = \frac{(L_i - L_f)}{L_i} * 100 \quad (3)$$

The flexural strength (FS) of the heated samples, was measured with a three-point bending method using a NETSZH global testing machine; the measurements are converted to flexural strength by applying Eq. (4)

$$FS = \frac{3}{2}\frac{E * d}{w * t^2} \quad (4)$$

where, E is the failure load (N), d is the distance between two supports (cm), w is the specimen width (cm) and t is the specimen thickness (cm).

## 3. RESULTS AND DISCUSSION

### 3.1 The melting behavior of SLGW and feldspar

Figure 2 shows the difference in the melting behaviour, in a tunnel kiln at 1230°C, between sodium and potassium feldspar on one side, and SLGW on the other. SLGW has a fast-melting behavior compared with both types of feldspar, because of the high presence of the liquid phase, which reduces the sintering process. The liquid phase formed in the matrix of ceramic specimens with added SLGW which consist of a great amount of diverse fluxes (such as CaO, $K_2O$ and $Na_2O$). While each type of feldspar has only one flux ($K_2O$, $Na_2O$ or CaO) [29].

### 3.2 The effect of SLGW on the rheological parameters of slip

According to the results given in Table 4, the rheological parameters of slip (such as viscosity, thixotropy and density) are consistent with the known existing ranges of values of VC ceramics; also, the sieve residue and thickness values are in the reported range. Generally, the slip does not need most of the used deflocculates agents, when incorporating SLGW in ceramic composition; The viscosity of the slip greatly affects the surface charge of the ceramic particles, therefore, allowing a change in the pH [30]. So, the addition of SLGW contributes to the formation of sodium and calcium hydroxides by the excessive amount of Na+ and Ca+ cations in the medium, which reduces the thickness of the diffusion layer [31].

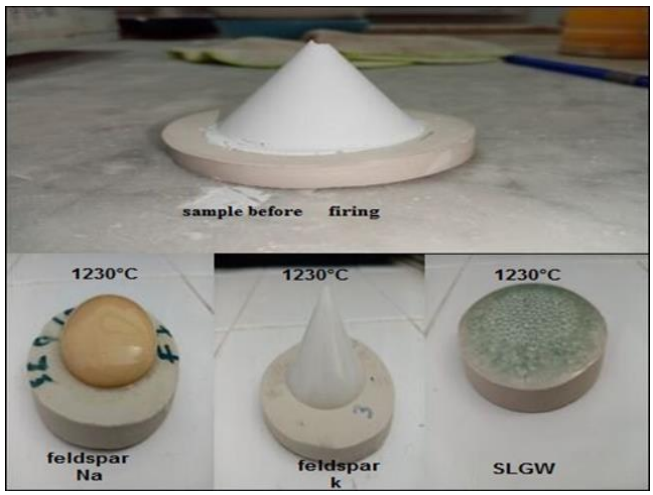


**Figure 2.** Melting of feldspar and SLGW at 1230 ºC

**Table 4.** Rheological properties of slip compositions

| | VC | C2 | C3 | C4 | C5 |
|---|---|---|---|---|---|
| Slip density (g/cm$^3$) | 1.77 | 1.78 | 1.78 | 1.77 | 1.78 |
| Fluidity (s) | 16 | 14 | 11 | 12 | 11 |
| Residue on sieve (63µm) | 1.7 | 1.9 | 1.8 | 1.5 | 1.9 |
| Viscosity (°G) | 300 | 305 | 309 | 299 | 300 |
| Drying shrinkage (%) | 4.11 | 7.19 | 7.87 | 7.98 | 8.30 |
| Thixotropy after 5 min (°G) | 52 | 32 | 9 | 15 | 10 |
| Thixotropy after 15 min (°G) | 87 | 55 | 22 | 19 | 17 |
| Thickness after 1 h (mm) | 6.7 | 7.8 | 6.50 | 6.80 | 6.10 |
| Sodium silicate deflocculated (%) | | | 0.1 | | |
| Sodium carbonate deflocculated (%) | | | 0.075 | | |

### 3.3 The effect of SLGW on the physical properties of fired ceramics

Figure 3 and Figure 4 present the results for the bulk density, total porosity, water absorption and firing shrinkage of fired ceramics. The addition of SLGW to the composition of ceramic bodies contributed to a significant reduction in the porosity of industrial VC ceramic, which has a higher total porosity of>10% compared to the sample containing 20 wt. % SLGW (2.8%). While the increase in density (up to 2.52 g/cm$^3$), is due to the liquid phase formation from various fluxes of SLGW (CaO and $Na_2O$). The liquid phase fills the voids between the substance's particles and leads to the decrease in the pores in the ceramic structure; this contributes to the conversion of the remaining open porosity to closed porosity, causing a decrease in the total volume of the sample (increase in the linear shrinkage) and reduction in the water absorption [32]. According to ASTM C 373-88 [33], all samples have a final shrinkage smaller than 12%. It must be noted that low water absorption (<0.5%) is essential to guarantee hygiene all along the product's lifetime. These results confirm that density is related to properties such as porosity, water absorption and linear shrinkage [34].

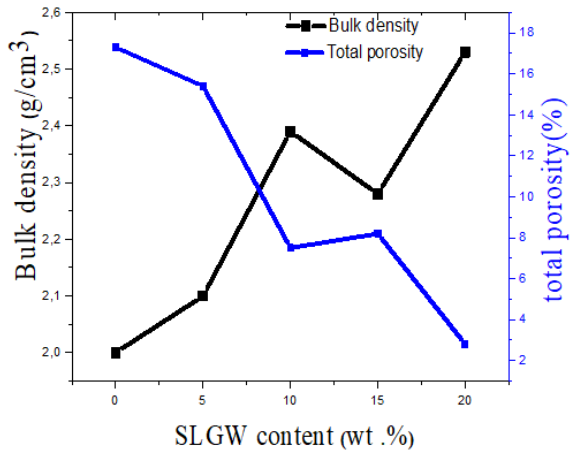


**Figure 3.** Bulk density and total porosity of the sintered samples

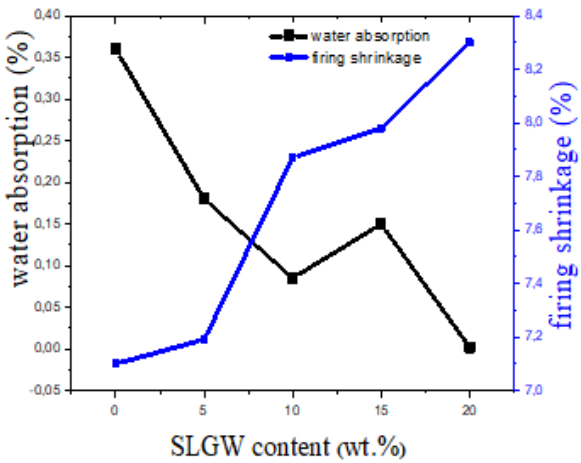


**Figure 4.** Water absorption and firing shrinkage of the sintered samples

### 3.4 Effect of SLGW on flexural strength of fired samples

Figure 5 shows the flexural strength variation of fired samples. The sample C5 has a high strength (51 MPa) compared to standard VC ceramic (33 MPa). We can notice, also, slight increase in the flexural strength of samples C2, C3 and C4, where we have SLGW incorporation. This increase can be explained by the difference in thermal expansion coefficient between glass matrix, mullite, quartz and grains of anorthite formed; as they contribute to a higher prestressing during the cooling process [7, 35]. In the C4 samples, the flexural strength decreased compared to C3; which can be attributed to the presence of a high amount of low-density liquid phase that leads to a bulging of the ceramic samples. These results are consistent with SEM analyses, which show a relatively higher porosity in C4 compared to C3 [32].

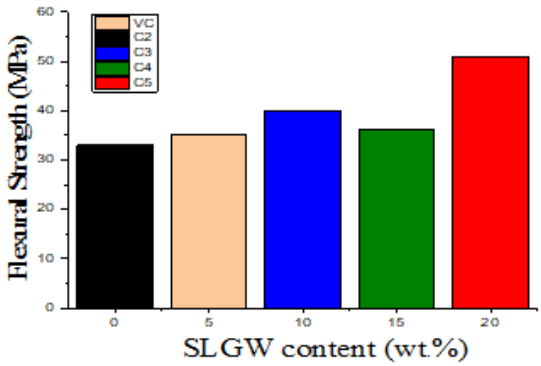


**Figure 5.** Evolution of the flexural strength of samples fired at 1230°C

### 3.5 X-ray diffraction analysis

Figure 6 presents the XRD analysis of samples fired at 1230°C. Mullite and quartz appear to be the main phases. SLGW incorporation in ceramic formulations leads to the formation of the anorthite phase. The presence of a sharp point in all samples is attributed to the presence of quartz as the predominant element in a crystalline state. The five ceramic samples contain an amount of $SiO_2$ >70% (Table 3) from undissolved quartz in raw materials [16]. The combination of alkaline and alkaline earth, contribute to the formation of mullite and glass phase while, the presence of CaO >13% in SLGW powder, leads to anorthite formation [36, 37].

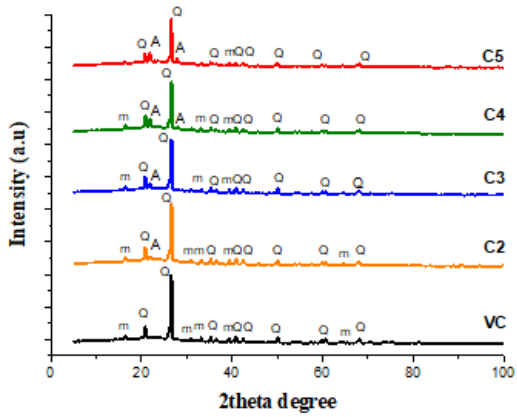


**Figure 6.** XRD pattern of heated samples. (m: mullite, Q: quartz, A: anorthite)

### 3.6 Scanning Electron Microscopy (SEM)

The microstructure of samples fired at 1230°C is shown in

Figure 7. Usually, VC bodies consist of mullite, quartz, and a liquid phase from molten clay-feldspar; SLGW has various fluxes (such as CaO, MgO, $K_2O$ and $Na_2O$) which lead to the formation of a great amount of liquid phase that fills the voids between the particles leading to a reduction in porosity of C2, C3, C4 and C5 samples. It is, also, found that the grain distribution in bodies containing SLGW, is similar to that of the standard VC sample [2]. According to the X-ray diffraction pattern shown in Figure 5, these samples contain also the anorthite phase formed by CaO oxide from SLGW powder. These results are consistent with physical parameters recorded previously such as density and water absorption.

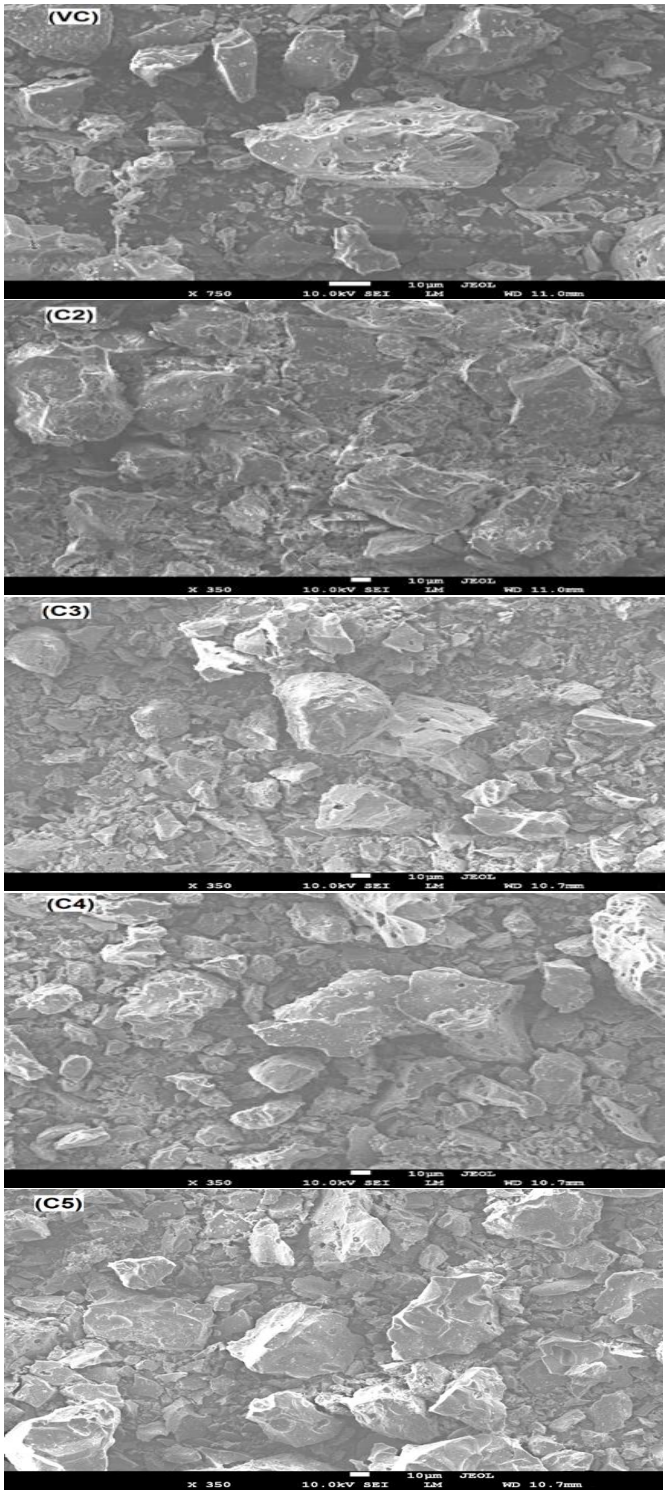


**Figure 7.** SEM micrographs of VC body and C2, C3, C4 and C5 ceramics

### 3.7 Thermal analysis

From TGA curves in Figure 8, Figure 9 and Figure 10, in three samples we can see a first mass loss in the interval 20°C - 100°C, corresponding to water elimination. The second mass loss between 400 and 600°C, is due to the dehydroxylation of the hydroxyl groups in kaolin resulting to form metakaolin ($A1_2O_3.2SiO_2$); that is confirmed by DTG analysis showing the apparent peaks at 480°C for VC sample and 500°C for samples containing 5 and 15 wt. % SLGW [38]. The mass loss continues as the temperature is raised; indeed, DTG analysis shows three small peaks at 1099, 1047 and 1107°C for 0, 5 and 15 wt.% SLGW, respectively. This is related to mullite formation by crystallization [7]. The total mass loss values in the mixtures 0, 5, and 15 wt. % SLGW are: 8.83, 8.12 and 8.56%, respectively. SLGW reduces mass loss in sanitary VC bodies by the formation of the liquid phase from the SLGW component. This mechanism has to do with the dissolution of the solids in the liquid phase and growth of crystalline phases (mullite) [29, 39].

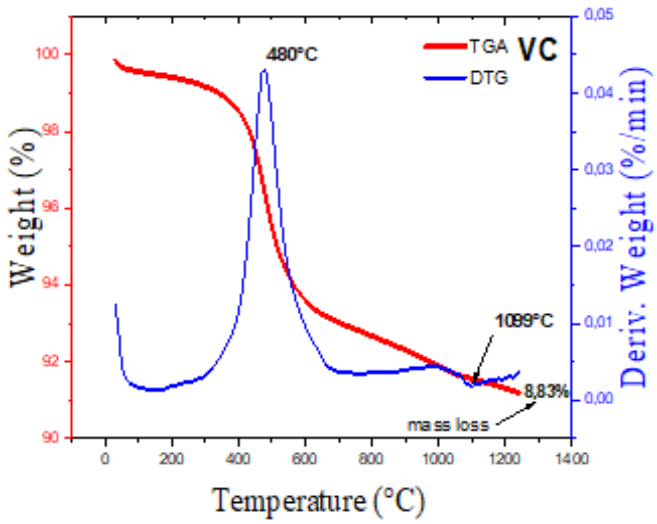


**Figure 8.** TGA/DTG analysis of the mixture, with 0% of SLGW

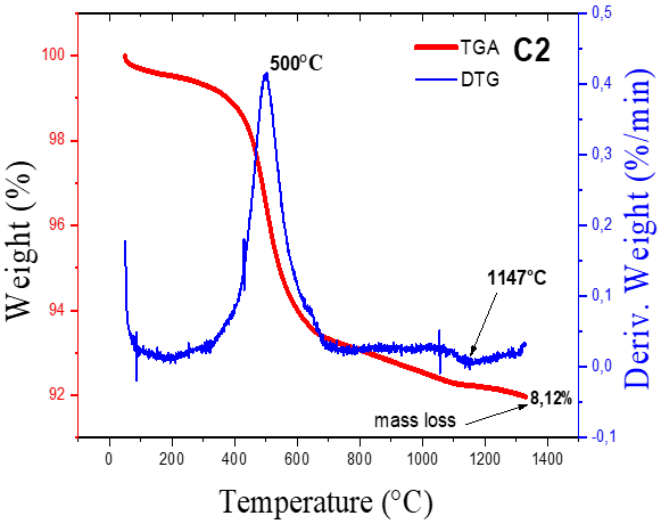


**Figure 9.** TGA/DTG analysis of the mixture, with 5% of SLGW

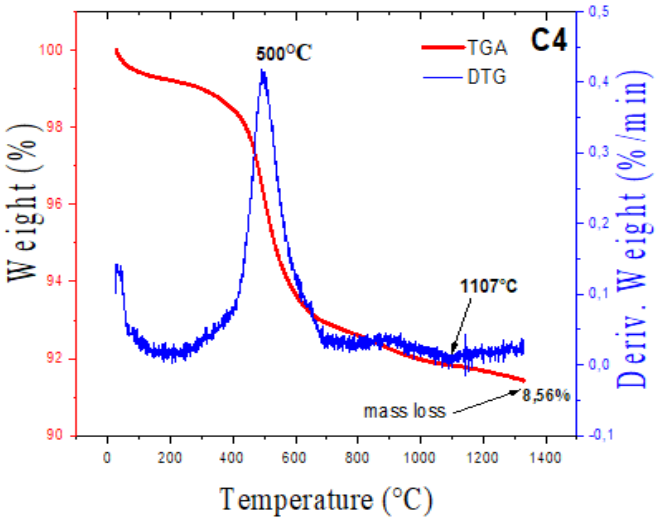


**Figure 10.** TGA/DTG analysis of the mixture, with 15% of SLGW

### 3.8 FTIR spectroscopy

In Figure 11, the FTIR spectra of the studied ceramics are presented. It shows that most bands are narrow, confirming the regular structure of the ceramic samples. The peak at 715 $cm^{-1}$ can be attributed to the bending vibration mode of (Al-O-Si) bonds [40]. The band appearing near 1079 $cm^{-1}$, could be due to Si-O vibrations and (Si-O-Si) asymmetric stretching vibration of siloxane bonds [41]. The small band at 1580$cm^{-1}$ could be caused by the C=O stretching frequency [42, 43]. The sharp bands at 2352$cm^{-1}$ could be ascribed to Si-C stretching [41]. The very small bands that appear at 3232$cm^{-1}$ in samples containing SLGW, indicate the absorption of calcium silicate hydrate compounds (Ca-Si-H) [44].

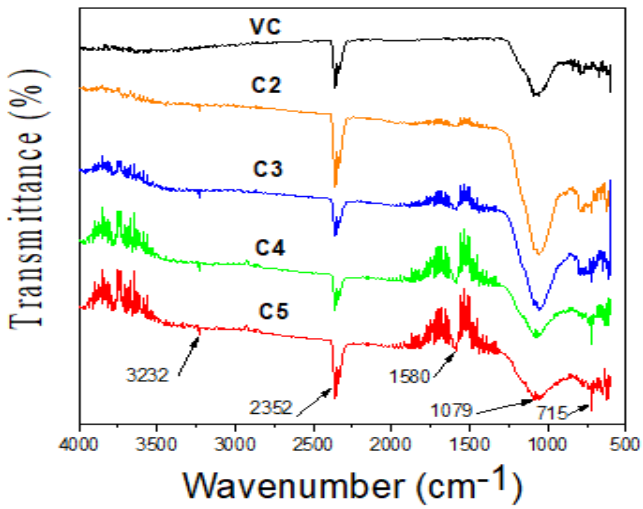


**Figure 11.** FTIR analysis of the mixtures with 0, 5, 10, 15and 20 % SLGW

## 4. CONCLUSIONS

Sanitary VC ceramics have been produced from soda-lime glass waste using the slip method. SLGW powder has been found enhance the rheological behavior of the slip. The use of SLGW (20 wt. %) has improved physical properties such as, bulk density (2 -2.52 g/$cm^3$), reduced water absorption (0.35 to 0.02%), and enhances the flexural strength (33-51 MPa). FTIR and XRD results, identified mullite and quartz as major crystalline phases with a little presence of anorthite following SLGW additions. SEM analysis shows a high density in samples rich in SLGW and a higher growth speed of mullite; this leads to the decreasing of porosity and water absorption. From TGA/DTG analysis, the substitution of feldspar by SLGW, has reduced the mass loss (8.83 to 8.53%) in VC ceramics containing 15wt. % SLGW. Finally, the results of this research, suggest that it is possible to produce sanitary ceramic VC bodies at a low cost from waste glass, as an alternative to feldspar, with many technical, environmental and economic benefits.

## ACKNOWLEDGMENT

The authors acknowledge that the LEAM laboratory of Jijel University and sanitary ceramic company of El-Milia-Algeria, provided as with the necessary assistance to complete this work.

## REFERENCES

[1] Silvestri, L., Forcina, A., Silvestri, C., Ioppolo, G. (2020). Life cycle assessment of sanitaryware production: A case study in Italy. Journal of Cleaner Production, 251: 119708. https://doi.org/10.1016/j.jclepro.2019.119708

[2] Gol, F., Yilmaz, A., Kacar, E., Simsek, S., Sarıtas, Z.G., Ture, C. (2021). Reuse of glass waste in the manufacture of ceramic tableware glazes. Ceramics International, 47: 21061-8. https://doi.org/10.1016/j.ceramint.2021.04.108

[3] Martini, E., Fortuna, D., Fortuna, A., Rubino, G., Tagliaferri, V. (2017). Sanitser, an innovative sanitary ware body, formulated with waste glass and recycled materials. Cerâmica, 63: 542-548. https://doi.org/10.1590/0366-69132017633682220

[4] Boudeghdegh, K., Diella, V., Bernasconi, A., Roula, A., Amirouche, Y. (2015). Composition effects on the whiteness and physical-mechanical properties of traditional sanitary-ware glaze. Journal of the European Ceramic Society, 35: 3735-3741. https://doi.org/10.1016/j.jeurceramsoc.2015.05.003

[5] Sun, S., Ding, H., Ao, W., Zhang, B., Liu, Y., Zhang, J. (2022). A zirconium-free glaze system for sanitary ceramics with $SiO_2$-$CaCO_3$-$TiO_2$ composite opacifier containing anatase: Effect of interface combination among $SiO_2$, $CaCO_3$ and $TiO_2$. Journal of the European Ceramic Society, 42: 2523-2534. https://doi.org/10.1016/j.jeurceramsoc.2021.12.069

[6] Naseem, M., Verma, R., Kango, S., Odakkel, M. (2020). Thermo-mechanical evaluation of slurry-sprayed multi-layered coatings. Arabian Journal for Science and Engineering, 45. https://doi.org/10.1007/s13369-020-04793-z

[7] Pal, M., Das, S., Gupta, S., Das, S.K. (2016). Thermal analysis and vitrification behavior of slag containing porcelain stoneware body. Journal of Thermal Analysis and Calorimetry, 124: 1169-1177. https://doi.org/10.1007/s10973-015-5179-7

[8] Martín-Márquez, J., Rincón, J., Romero, M. (2008). Effect of firing temperature on sintering of porcelain stoneware tiles. Ceramics International, 34: 1867-1873.

https://doi.org/10.1016/j.ceramint.2007.06.006
[9] Bernasconi, A., Diella, V., Pagani, A., Pavese, A., Francescon, F., Young, K. (2011). The role of firing temperature, firing time and quartz grain size on phase-formation, thermal dilatation and water absorption in sanitary-ware vitreous bodies. Journal of the European Ceramic Society, 31: 1353-1360. https://doi.org/10.1016/j.jeurceramsoc.2011.02.006
[10] Stathis, G., Ekonomakou, A., Stournaras, C.J., Ftikos, C. (2004). Effect of firing conditions, filler grain size and quartz content on bending strength and physical properties of sanitaryware porcelain. Journal of the European Ceramic Society, 24: 2357-2366. https://doi.org/10.1016/j.jeurceramsoc.2003.07.003
[11] Carty, W., Senapati, U. (2005). Porcelain—raw materials, processing, phase evolution, and mechanical behavior. Journal of the American Ceramic Society, 81: 3-20. https://doi.org/10.1111/j.1151-2916.1998.tb02290.x
[12] Olcoski, T., Chinelatto, A., Chinelatto, A. (2021). Effect of MgO addition on the sinterability and mechanical properties of mullite ceramics. Cerâmica, 67: 261-268. https://doi.org/10.1590/0366-69132021673833075
[13] Marinoni, N., Pagani, A., Adamo, I., Diella, V., Pavese, A., Francescon, F. (2011). Kinetic study of mullite growth in sanitary-ware production by in situ HT-XRPD. The influence of the filler/flux ratio. Journal of the European Ceramic Society, 31(3): 273-280. https://doi.org/10.1016/j.jeurceramsoc.2010.10.002
[14] Du, Y., Gao, J., Lan, X., Guo, Z. (2022). Preparation of TiC ceramics from hot Ti-bearing blast furnace slag: Carbothermal reduction, supergravity separation and spark plasma sintering. Journal of the European Ceramic Society, 42(5): 2055-2061. https://doi.org/10.1016/j.jeurceramsoc.2021.12.047
[15] Karamanova, E., Avdeev, G., Karamanov, A. (2011). Ceramics from blast furnace slag, kaolin and quartz. Journal of the European Ceramic Society, 31(6): 989-998. https://doi.org/10.1016/j.jeurceramsoc.2011.01.006
[16] El-Fadaly, E. (2013). Characterization of porcelain stoneware tiles based on solid ceramic wastes. International Journal of Science and Research (IJSR), 4(1): 602-608.
[17] Liang, X., Li, Y., Yan, W., Wang, Q., Tan, F., He, Z. (2021). Preparation of SiC reticulated porous ceramics with high strength and increased efficient filtration via fly ash addition. Journal of the European Ceramic Society, 41: 2290-2296. https://doi.org/10.1016/j.jeurceramsoc.2020.11.039
[18] Das, D., Kayal, N., Gabriel, A., Daniel, G., Innocentini, M. (2020). Recycling of coal fly ash for fabrication of elongated mullite rod bonded porous SiC ceramic membrane and its application in filtration. Journal of the European Ceramic Society, 40. https://doi.org/10.1016/j.jeurceramsoc.2020.01.034
[19] Chen, A.N., Li, M., Xu, J., Lou, C.H., Wu, J.M., Cheng, L. (2018). High-porosity mullite ceramic foams prepared by selective laser sintering using fly ash hollow spheres as raw materials. Journal of the European Ceramic Society, 38(13): 4553-4559. https://doi.org/10.1016/j.jeurceramsoc.2018.05.031
[20] Sglavo, V.M., Maurina, S., Conci, A., Salviati, A., Carturan, G., Cocco, G. (2000). Bauxite 'red mud'in the ceramic industry. Part 2: Production of clay-based ceramics. Journal of the European Ceramic Society, 20: 245-252. https://doi.org/10.1016/S0955-2219(99)00156-9
[21] Cocic, M., Matović, B., Pošarac, M.B., Volkov-Husović, T., Majstorovic, J., Tasic, V. (2017). Thermal shock properties of glass-ceramics synthesized from a glass frit. Science of Sintering, 49(2): 139-147. https://vinar.vin.bg.ac.rs/handle/123456789/1643
[22] Kim, K., Kim, K., Hwang, J. (2016). Characterization of ceramic tiles containing LCD waste glass. Ceramics International, 42: 7626-7631. https://doi.org/10.1016/j.ceramint.2016.01.172
[23] Hossain, S.S., Roy, P. (2020). Sustainable ceramics derived from solid wastes: A review. Journal of Asian Ceramic Societies, 1-26. https://doi.org/10.1080/21870764.2020.1815348
[24] Canakci, H., Güllü, H., Isam, M. (2018). Effect of glass powder added grout for deep mixing of marginal sand with clay. Arabian Journal for Science and Engineering, 43: 1583-95. https://doi.org/10.1007/s13369-017-2655-3
[25] Raut, A., Gomez, C. (2020). Utilization of glass powder and oil palm fibers to develop thermally efficient blocks. Arabian Journal for Science and Engineering, 45: 1-14. https://doi.org/10.1007/s13369-019-04316-5
[26] Rambaldi, E., Carty, W.M., Tucci, A., Esposito, L. (2007). Using waste glass as a partial flux substitution and pyroplastic deformation of a porcelain stoneware tile body. Ceramics International, 33(5): 727-733. https://doi.org/10.1016/j.ceramint.2005.12.010
[27] Bragança, S.R., Bergmann, C.P. (2005). Waste glass in porcelain. Materials Research, 8(1): 39-44.
[28] Matteucci, F., Dondi, M., Guarini, G. (2002). Effect of soda-lime glass on sintering and technological properties of porcelain stoneware tiles. Ceramics International, 28(8): 873-880. https://doi.org/10.1016/S0272-8842(02)00067-6
[29] Marinoni, N., D'Alessio, D., Diella, V., Pavese, A., Francescon, F. (2013). Effects of soda–lime–silica waste glass on mullite formation kinetics and micro-structures development in vitreous ceramics. Journal of Environmental Management, 124: 100-107. https://doi.org/10.1016/j.jenvman.2013.02.048
[30] El-Fadaly, E.A., Askar, A.S., Aly, M.H., Ibrahim, D.M. (2020). Rheological, physico-mechanical and microstructural properties of porous mullite ceramic based on environmental wastes. Boletín de la Sociedad Española de Cerámica y Vidrio. https://doi.org/10.1016/j.bsecv.2020.08.002
[31] Evcin, A. (2011). Investigation of the effects of different deflocculants on the viscosity of slips. Scientific Research and Essays, 6(11): 2302-2305. https://doi.org/10.5897/SRE10.686
[32] Salman, M.M., Nhabih, H.T. (2020). Assessment of the partial and total replacement of feldspar by waste glass on por-celain properties. Journal of Ceramic Processing Research, 21(3): 371-377.
[33] ASTM C373-88. (2006). Standard test method for water absorption, bulk density, apparent porosity, and apparent specific gravity of fired whiteware products. Glass and Ceramic, 15(2): 1-2.
[34] İssi, A., Derin Coşkun, N., Tiryaki, V., Uz, V. (2017). Casting and sintering of a sanitaryware body containing fine fire clay (FFC). Journal of the Australian Ceramic Society, 53(1): 157-162. https://doi.org/10.1007/s41779-016-0020-8

[35] Dana, K., Das, S.K. (2004). Partial substitution of feldspar by BF slag in triaxial porcelain: Phase and microstructural evolution. Journal of the European Ceramic Society, 24(15-16): 3833-3839. https://doi.org/10.1016/j.jeurceramsoc.2004.02.004
[36] Wang, S., Li, X., Wang, C., Bai, M., Zhou, X., Zhang, X., Wang, Y. (2022). Anorthite-based transparent glass-ceramic glaze for ceramic tiles: Preparation and crystallization mechanism. Journal of the European Ceramic Society, 42(3): 1132-1140. https://doi.org/10.1016/j.jeurceramsoc.2021.11.036
[37] Albhilil, A.A., Kozánková, J., Palou, M. (2014). Thermal and microstructure stability of cordierite–mullite ceramics prepared from natural raw materials. Arabian Journal for Science and Engineering, 39(1): 67-73. https://doi.org/10.1007/s13369-013-0863-z
[38] Anggono, J. (2005). Mullite ceramics: its properties structure and synthesis. Jurnal Teknik Mesin, 7(1): 1-10.
[39] Boussak, H., Chemani, H., Serier, A. (2015). Characterization of porcelain tableware formulation containing bentonite clay. International Journal of Physical Sciences, 10(1): 38-45. https://doi.org/10.5897/IJPS2014.4218
[40] Zawrah, M.F., Gado, R.A., Khattab, R.M. (2018). Optimization of slag content and properties improvement of metakaolin-slag geopolymer mixes. The Open Materials Science Journal, 12(1).
[41] Joni, I.M., Nulhakim, L., Vanitha, M., Panatarani, C. (2018). Characteristics of crystalline silica ($SiO_2$) particles prepared by simple solution method using sodium silicate ($Na_2SiO_3$) precursor. In Journal of Physics: Conference Series, 1080(1): 012006. https://doi.org/10.1088/17426596/1080/1/012006
[42] Zakaly, H.M., Saudi, H.A., Tekin, H.O., Rashad, M., Issa, S.A., Rammah, Y.S., Ene, A. (2021). Glass fabrication using ceramic and porcelain recycled waste and lithium niobate: physical, structural, optical and nuclear radiation attenuation properties. Journal of Materials Research and Technology, 15: 4074-4085. https://doi.org/10.1016/j.jmrt.2021.09.138
[43] Michailova, I., Radev, L., Aleksandrova, V., Colova, I., Salvado, I., Fernandes, M. (2015). Carbonate-apatite forming ability of polyphase glass-ceramics in the CaO - MgO - $SiO_2$ system. Journal of Chemical Technology and Metallurgy, 50(4): 502-511.
[44] Monich, P.R., Romero, A.R., Höllen, D., Bernardo, E. (2018). Porous glass-ceramics from alkali activation and sinter-crystallization of mixtures of waste glass and residues from plasma processing of municipal solid waste. Journal of Cleaner Production, 188: 871-878. https://doi.org/10.1016/j.jclepro.2018.03.167